



## Novel Ultrahard Carbon Allotrope $C_5$ with Mixed $sp^2/sp^3$ Carbon Hybridizations. Crystal chemistry and First Principles Investigations

Samir F Matar\*

Lebanese German University (LGU), Sahel-Alma, Jounieh, Lebanon

\*Corresponding Author: Samir F Matar, Lebanese German University (LGU), Sahel-Alma, Jounieh, Lebanon. Email: sfm68@hotmail.com

Received: November 28, 2022

Published: December 06, 2022

© All rights are reserved by Samir F Matar.

### Abstract

From crystal chemistry rationale and first principles investigations, novel tetragonal carbon allotrope  $C_5$  with mixed  $sp^2/sp^3$ -like carbon sites hybridizations is identified as cohesive and stable both dynamically and mechanically with metallic behavior. Charge density distribution is localized at tetrahedral C- $sp^3$  and delocalized with  $\pi$ -like electrons between trigonal C- $sp^2$  leading to metallic like electronic behavior. The anisotropic structure resulting from vertically aligned C=C (ethene-like) along the tetragonal c-axis provides large  $C_{33}$  elastic constant and high Vickers hardness with a magnitude slightly below diamond. The properties of novel simple allotrope should help assessing nanodiamonds with mixed  $sp^2/sp^3$  C investigated in different fields of materials as electrochemical ones.

**Keywords:** Diamond; Hardness; Phonons; DFT; Crystal Chemistry

### Introduction

Diamond is recognized as the hardest material [1]. In last decades large research efforts were devoted to identifying novel allotropes of carbon close to diamond using modern materials research methodologies as CALYPSO [2]. In view of the large number of claimed stoichiometries and structures, a database: SACADA was built regrouping all known carbon allotropes to help researchers and to avoid erroneous claims of existing systems [3].

Recently published body centered tetragonal BCT  $C_4$  (Figure 1a) was proposed in space group I-4m2 as one of the simplest three-dimensional (3D) carbon networks with ultra-hard properties [4]. It was then found out that by considering the primitive cell,  $C_4$  had the same topology as cubic diamond using TopCryst crystallography package [5] with "dia" -for diamond- topology as categorized for several chemical compounds in Reticular Chemistry Structure Resource (RCSR) Database [6]. Nevertheless, with its simplicity BCT  $C_4$  can be used as seed-template for other original chemical compounds as shown herein. Starting from  $C_4$ , novel tetragonal  $C_5$  is built through crystal chemistry followed by full geometry relax-

ations using calculations based on the quantum mechanics density functional theory DFT [7]. Analyzed through TopCryst crystallography program, the fully geometry relaxed structure of  $C_5$  was found to be in original uncategorized topology within RCSR Database [6]. The novel allotrope found cohesive and stable both mechanically and dynamically is characterized with large hardness magnitude slightly below diamond. Furthermore,  $C_5$  has mixed carbon hybridization  $sp^2$  and  $sp^3$ . Such stoichiometry and chemical behavior were reported in recent literature for so-called cubic 'pentadiamond', qualified as a novel allotrope with high mechanical properties close to diamond; but the paper was later retracted due to calculation errors on the mechanical properties admitted by the authors [8]. The relevance of mixed carbon hybridization is in the change of the mechanical properties of the hardest material, diamond, and of its electronic insulating structure.

The relevance of mixed carbon hybridization bringing changes of the electronic structure of insulating diamond by inducing metallic-like behavior. Such modifications lead to applications in materials science. As a matter of fact, mixed C( $sp^2$ )/C( $sp^3$ ) were identi-

fied in nanodiamonds, arising large interest in different fields of materials investigations as electrochemical ones recently exposed by Zhai, *et al.* [9]. The presently proposed original Pentacarbon is meant to serve as a model illustrating the observed electronic, mechanical, and dynamic behaviors at an elementary scale of small cluster made of 3  $C(sp^3)$  and 2  $C(sp^2)$ .

### Computational framework

The search for the ground state structures goes through protocols of geometry optimizations calculations onto the ground state characterized by minimal energies. The iterative computations were performed using DFT-based plane-wave Vienna Ab initio Simulation Package (VASP) [10,11]. For the atomic potentials, the projector augmented wave (PAW) method was used [11,12]. DFT exchange and correlation effects (XC) were treated locally at the same level with a generalized gradient approximation scheme (GGA) [13]. The relaxation of the atoms onto ground state geometry was done applying a conjugate-gradient algorithm [14]. A tetrahedron method [15] with corrections made with Methfessel-Paxton scheme [16] was applied for geometry optimization and energy calculations, respectively. A special  $k$ point sampling [17] was applied for approximating the reciprocal space Brillouin-zone (BZ) integrals. For better reliability, the optimization of the structural parameters was carried out along with successive self-consistent cycles with increasing mesh until the forces on atoms were less than  $0.02 \text{ eV/\AA}$  and the stress components below  $0.003 \text{ eV/\AA}^3$ .

The mechanical stabilities and hardness were inferred from the calculations of the elastic constants. Furthermore, the phonon dispersion band structures were calculated to verify the dynamic stability of the novel carbon allotropes. The phonon modes were computed considering the harmonic approximation through finite displacements of the atoms around their equilibrium positions to obtain the forces from the summation over the different configurations. The phonon dispersion curves along the direction of the Brillouin zone were subsequently obtained using "Phonopy" interface code based on Python language [18].

The electronic band structures and density of states were obtained with the full-potential augmented spherical wave ASW method based on DFT using the same GGA scheme as above [19].

	$C_4$ [4] I-4m2, N°119	$C_3$ P-4m2, N°115	$C_5$ P-4m2, N°115
a	2.527	2.521	2.4786
c	3.574	3.402	5.0279
C1(tet.)	(2a) 0, 0, 0	(1a) 0, 0, 0	(1a) 0, 0, 0
C2(tet.)	(2d) $\frac{1}{2}$ , 0, $\frac{1}{4}$	(2g) $\frac{1}{2}$ , 0, z z= 0.237	(2g) $\frac{1}{2}$ , 0, z z= 0.187
C(trig.)	-	-	(2f) $\frac{1}{2}$ , $\frac{1}{2}$ , z z= 0.646
Volume ( $\text{\AA}^3$ )	22.82	21.63	30.89
$d_{C1(tet.)-C2(tet.)}$	1.55	1.50	1.55
$d_{C2(tet.)-C2(trig.)}$	-	-	1.50
$d_{C(trig.)-C(trig.)}$	-	-	1.46
$E_{total}$	-36.36	-21.58	-43.26
$E_{coh./at.}$	-2.49	-0.59	-2.05

**Table 1:** Tetragonal carbon crystal structure parameters:  $C_4$ ,  $C_3$ , and  $C_5$ . Lattice constants and distances are in units of  $\text{\AA}$  (Vol.  $\text{\AA}^3$ ).

Energies are in eV.

### Crystal chemistry and characteristics of $C_5$

Body center tetragonal  $C_4$  structure (Figure 1a) consists of two distinct carbon sites with 2-atoms occupancy: C1 at the corner and body center positions developing  $C_4$  tetrahedra with C2 positioned at the faces (Table 1a). We highlight that all lattice parameters of the structures in Table 1 result from unconstrained geometry optimizations to the energy ground states. The removal of the body center carbon breaks the body-center symmetry and leads to  $C_3$  where tetrahedra are at the 8 corners forming a two-dimensional like stacking along c-tetragonal direction (Figure 1b). Such modification leads to a lowering of symmetry and the space group shifts from I-4m2, N°119 down to P-4m2, N°115. The second column of Table 1 shows  $C_3$  crystal parameters with the Wyckoff positions. Both types of carbon atoms are labeled C1(tet) and C2(tet) in so far that they produce tetrahedral carbon. Expectedly, the volume and the interatomic distance decrease with the removal of one carbon. The last lines present the total energy and the atom averaged cohesive energies. From the cohesive energy there is a large destabilization of the diamond-like structure upon removal of central carbon to create  $C_3$  that can be used as template to devise novel allotropes.

It needs to be noted that despite the small magnitude cohesive energy (Table 1) -versus the other allotropes in Table 1,  $C_3$  was found mechanically and dynamically stable from the sets of elastic constants and phonons band structures respectively, as detailed in the development of the paper.

Consequently, the following scheme is presented:

$C_3$  “receives”

- One extra carbon to make  $C_4$ , already investigated [4],
- C-C pair to make  $C_5$  (shown in Figure 1c),
- One additional carbon atom at cell center, based on  $C_5$ , to make  $C_6$  introducing tricarbon entity, not developed upon here, and published as a structure in CCDC [20].

The major difference between  $C_4$  and  $C_5$  is that whereas in  $C_4$  the central carbon is tetrahedral C(tet) completing the diamond-like structure as discussed above, the two additional carbon atoms are labeled C(trig); with “trig” standing for trigonal carbon shown with white spheres in Figure 1c. Alike  $C_3$ , the new allotrope  $C_5$  belongs to P-4m2,  $N^\circ 115$  space group. The C-C interatomic distances are within range of  $C_4$  (diamond-like) and smaller magnitudes are observed for  $d(C_{\text{trig}}-C_{\text{trig}}) = 1.47 \text{ \AA}$ . Beside C-C single bonds for C(tet)-C(tet), we are in presence of additional double C=C bond, thus characterizing pentacarbon  $C_5$  with  $sp^2/sp^3$  carbon hybridizations. The atom averaged cohesive energy is significantly larger than in  $C_3$  with a magnitude close to  $C_4$ .

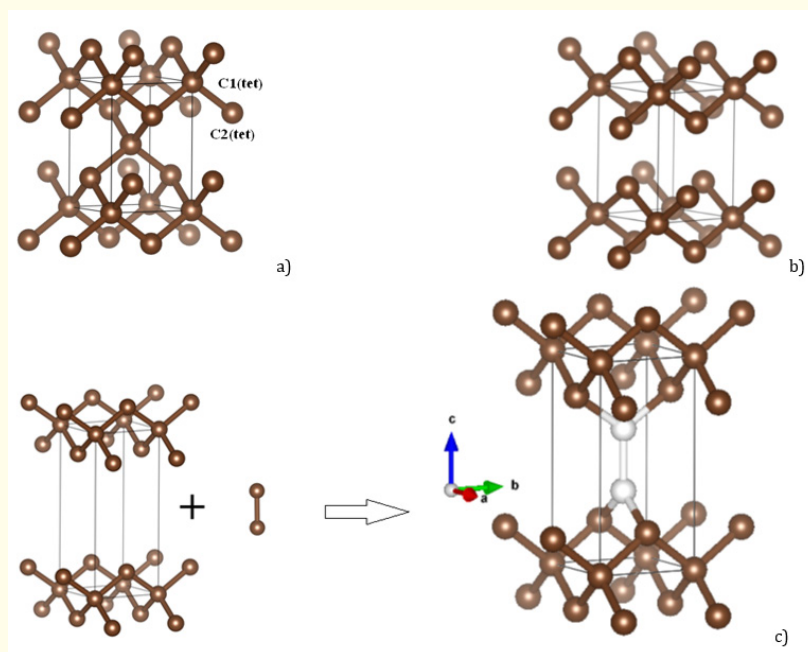


**Figure 1:** Sketches of the crystal structures with schematics of transformations (cf. text). a)  $C_4$ , b)  $C_3$ , and c)  $C_5$  White spheres represent trigonal carbon pair.

### Charge density projections

Further qualitative illustration of the different types of hybridizations is obtained from the projections of the charge densities around and between atoms. Figure 2 presents the projections shown with yellow volumes. Upon crossing crystal plane, charge density slices with red color are shown indicating strong charge localizations.

In  $C_4$  (Figure 2a) the  $sp^3$ -type hybridization expected for C(tet) is clearly observed especially on central carbon with the yellow volumes taking the shape of a tetrahedron, and alike diamond,  $C_4$  is a perfectly covalent chemical system. Upon removal of central carbon producing  $C_3$  with only C(tet) -cf. Table 1, the charge density is modified especially for the carbon atoms pointing towards the empty space as it is exhibited by the larger red area versus  $C_4$ .

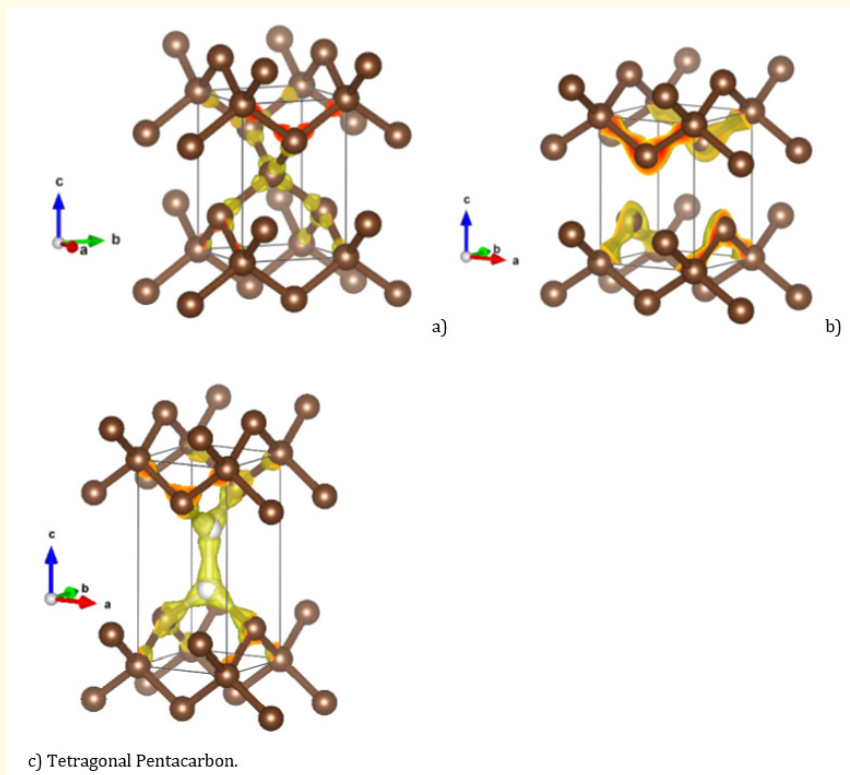


**Figure 2:** Charge density projections (yellow volumes) in a)  $C_4$ , b)  $C_3$ , and c)  $C_5$ . White spheres represent trigonal C=C (ethene-like) carbon pair.

Larger changes are observed in  $C_5$  (Figure 2c) where the charge density is skewed towards the ethene-like C=C pair of C(trig) white spheres. The charge density is no more homogeneously distributed as in covalent  $C_4$ , and less pronounced red color is observed letting suggest a polar-covalent behavior normally found in a compound with different constituents' electronegativities such as boron nitride.

Therefore, we are presented with a decrease of the covalence from  $C_4 \rightarrow C_5$  brought by the introduction of trigonal carbon.

### Mechanical properties from elastic constants

The investigation of mechanical properties was based on the calculations of the elastic properties determined by performing finite distortions of the lattice and deriving the elastic constants from the strain-stress relationship. Most compounds are polycrystalline, and generally considered as randomly oriented single crystalline grains. Consequently, on a large scale, such materials can be consid-

ered as statistically isotropic. They are then fully described by bulk (B) and shear (G) moduli obtained by averaging the single-crystal elastic constants. The method used here is Voigt's [21], based on a uniform strain. The calculated sets of elastic constants are given in Table 2; the elastic constants of  $C_4$  [6] are reported for the sake of comparison. While most elastic constants of  $C_4$  are larger than in  $C_5$ , it can be noted that  $C_{33}$  magnitude is larger in  $C_5$ , concomitantly with aligned trigonal C-C along the c-tetragonal axis (cf. Figure 1c).

The elastic constants of  $C_3$  exhibit a relatively large magnitude for in-plane  $C_{11}$  and much smaller magnitude for  $C_{33}$  relevant to inter-planes, i.e., along tetragonal c-direction. Both largest  $C_{ii}$  ( $C_{11}$  and  $C_{33}$ ) are smaller than the corresponding values in  $C_5$ . Indeed, the system describing  $C_3$  is more relevant to two-dimensional 2D letting it receive interstitials as schematized in Section 3, and hence leading to 3D  $C_4$ ,  $C_5$  and  $C_6$  etc. All magnitudes of the other  $C_{ij}$  are very small letting expect a soft material. However, it will be shown

that C<sub>3</sub> is dynamically valid from the calculations of positive phonon frequencies in next section.

	C <sub>11</sub>	C <sub>12</sub>	C <sub>13</sub>	C <sub>33</sub>	C <sub>44</sub>	C <sub>66</sub>	B <sub>Voigt</sub>	G <sub>Voigt</sub>
C <sub>4</sub> [4]	1147	28	126	1050	461	559	434	574
C <sub>5</sub>	922	21	112	1192	217	370	390	430
C <sub>3</sub>	696	20	33	155	10	5	191	115

**Table 2:** Calculated elastic constants and bulk B<sub>v</sub> and shear G<sub>v</sub> moduli. All values are in GPa units.

All C<sub>ij</sub> (i=j and i≠j) values are positive and their combinations obey rules pertaining to the mechanical stability of the chemical system.

$$C_{ii} \text{ (i=1, 3, 4, 6)} > 0; C_{11} > C_{12}, C_{11} + C_{33} - 2C_{13} > 0; \text{ and } 2C_{11} + C_{33} + 2C_{12} + 4C_{13} > 0.$$

The equations providing the bulk B<sub>v</sub> and shear G<sub>v</sub> moduli are as follows for the tetragonal system [22]:

$$B_{Voigt}^{tetr.} = 1/9 (2C_{11} + C_{33} + 2C_{12} + 4C_{13});$$

and

$$G_{Voigt}^{tetr.} = 1/15 (2C_{11} + C_{12} + 2 C_{33} - 2C_{13} + 6C_{44} + 3C_{66}).$$

C<sub>4</sub> has the largest B<sub>v</sub> and G<sub>v</sub>, close to the accepted values for diamond B<sub>v</sub>=445 GPa and G<sub>v</sub> = 550 GPa [1]. The corresponding B<sub>v</sub> and G<sub>v</sub> magnitudes in C<sub>5</sub> are slightly smaller but they remain high, oppositely to C<sub>3</sub> which shows much smaller B<sub>v</sub> and G<sub>v</sub> magnitudes versus C<sub>5</sub>.

Vickers hardness (H<sub>v</sub>) was predicted using three theoretical models of hardness [23-25]. The thermodynamic model (T) [23] is based on thermodynamic properties and crystal structure, while Mazhnik-Oganov (MO) [24] model uses the elastic properties. Lyakhov-Oganov (LO) approach [25] considers topology of the crystal structure, strength of covalent bonding, degree of ionicity and directionality. The fracture toughness (K<sub>ic</sub>) was evaluated within MO model [24].

The results are summarized in Table 3 presenting Vickers hardness calculated using the different theoretical models and other mechanical properties such as shear modulus (G), Young's modulus (E), the Poisson's ratio (ν) and fracture toughness (K<sub>ic</sub>). The hardness of tet.C<sub>4</sub> shows expectedly close magnitude to

	HV			B <sub>v</sub>	G <sub>v</sub>	E*	ν*	K <sub>ic</sub>
	T [23]	LO [24]	MO [25]					
C <sub>4</sub>	97	89	110	434	574	1195	0.041	6.4
C <sub>5</sub>	89	81	76	390	414	917	0.108	5.1
C <sub>3</sub>	--	26	13	191	115	287	0.249	2.0
Diamond	98	90	100	445 [1]	530 [1]	1138	0.074	6.4

**Table 3:** Mechanical properties of carbon allotropes: Vickers hardness (H<sub>v</sub>), bulk modulus (B), shear modulus (G), Young's modulus (E), Poisson's ratio (ν). All values are in GPa (Giga Pascal) unit. Fracture toughness (K<sub>ic</sub>) is in MPa·m<sup>½</sup>.

\*E and ν values calculated using isotropic approximation.

diamond using the three models as discussed in the introduction highlighting the close relationship of C<sub>4</sub> with diamond. Turning to C<sub>3</sub> low hardness magnitudes are identified with both LO and MO model while the thermodynamic model was found to provide unreliable values; nevertheless, with H<sub>v</sub> = 15 GPa tet-C<sub>3</sub> is described as a soft material. Lastly for tet-C<sub>5</sub> the thermodynamic model provides the highest hardness magnitude versus LO and LO models; all values are lower than in tet-C<sub>4</sub> or diamond due to the mixed valence carbon sites leading to less covalence than in ideal diamond. Concomitantly the fracture toughness: K<sub>ic</sub>(tet-C<sub>5</sub>) = 5.1 MPa·m<sup>½</sup> is found smaller than calculated for diamond with K<sub>ic</sub> = 6.4 MPa·m<sup>½</sup>. Lastly E and ν calculated with the isotropic approximation show lower magnitudes than diamond. Consequently, the novel pentacarbon allotrope can be considered as prospective ultra-hard material showing interesting mixed carbon hybridization.

### Dynamic properties from the phonons

Another criterion of stability is obtained from the phonons defined as quanta of vibrations; their energy is quantized through the Planck constant 'h' used in its reduced form ħ (ħ = h/2π) giving with the wave number ω the phonons energy: E = ħω. Besides the novel allotropes C<sub>3</sub> and C<sub>5</sub> the phonon band structures of C<sub>4</sub> [4] are shown for the sake of comparison. Figure 3 shows the phonon bands.

Along the horizontal direction, the bands run along the main lines of the tetragonal Brillouin zone (reciprocal k- space). The vertical direction shows the frequencies given in units of terahertz (THz). Since no negative frequency magnitudes are observed, ex-

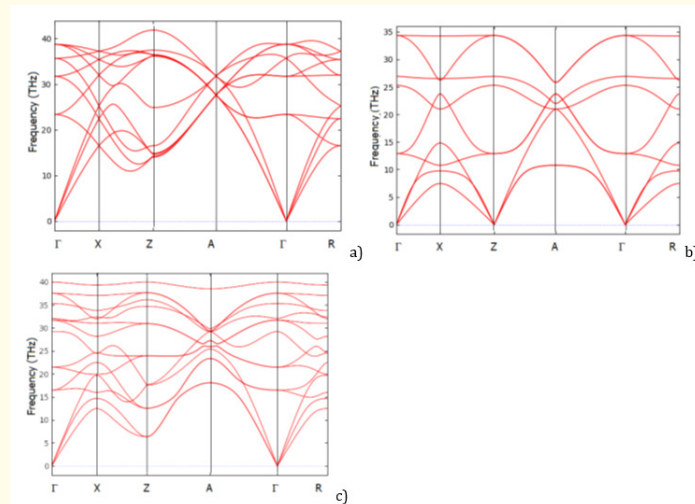


**Figure 3:** Phonons band structures of a)  $C_4$  [4], b)  $C_3$ , and c)  $C_5$ .

pectedly for  $C_4$ , but also for  $C_3$  and  $C_5$ , all structures are considered as dynamically stable. There are 3N-3 optical modes found at higher energy than three acoustic modes that start from zero energy ( $\omega = 0$ ) at the  $\Gamma$  point, center of the Brillouin Zone, up to a few Terahertz. They correspond to the lattice rigid translation modes of the crystal (two transverse and one longitudinal). The remaining bands correspond to the optic modes and culminating at  $\omega \sim 40$  THz in  $C_4$  and  $C_5$ , a magnitude observed for diamond by Raman spectroscopy [26], and only up to 34 in less stable  $C_3$  (cf. Table 1). The phonons show the closeness of  $C_5$  to  $C_4$  regarding dynamic stability.

### Electronic band structures and density of states

Using the crystal parameters in Table 1, the electronic band structures were obtained using the all-electrons DFT-based augmented spherical method (ASW) [19] and shown in Figure 4. The bands develop along the main directions of the primitive tetragonal Brillouin zones. For diamond-like insulating  $C_4$  (Figure 4a) the energy level along the vertical line is with respect to the top of the valence band (VB),  $E_v$ . As a specific character of diamond, the band gap of  $C_4$  is indirect along  $k_z$  between  $\Gamma_{VB}$  and  $Z_{CB}$  with a magnitude close to 5 eV. Oppositely,  $C_3$  (Figure 4b) and  $C_5$  (Figure 4c) behave as metals with bands crossing the Fermi level  $E_f$ .

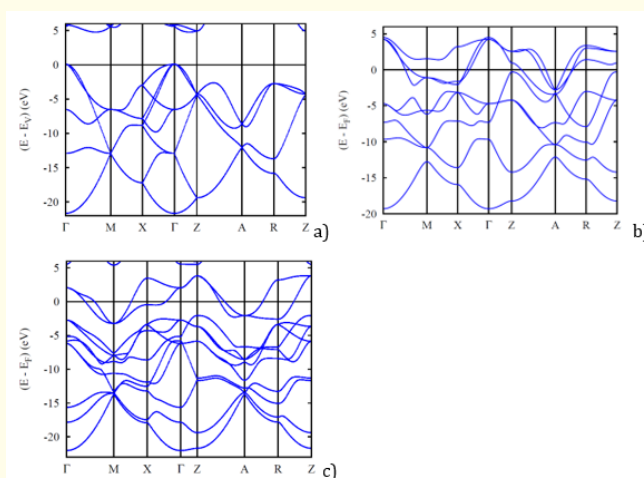


**Figure 4:** Electronic band structures of a)  $C_4$  [4], b)  $C_3$ , c)  $C_5$ .

### Concluding Note and Prospective

With novel  $C_5$  we are presented with a simple stoichiometry metallic material showing original occurrence of mixed  $sp^2$ - $sp^3$ -like carbon hybridizations, characterized by ultra-hardness close to diamond. The practical interest in such electronic systems is their presence in nanostructures of hybrid diamond/ $C(sp^2)$  inves-

tigated in the domain of electrochemistry, for instance.

As prospective work, extended 3D carbon networks are being examined to reduce the amount of C(sp<sup>2</sup>) to highlight further doping effect of diamond-like structures.

### Acknowledgments

I am grateful to Dr Vladimir Solozhenko Directeur de Recherche at CNRS-Paris for exchanges and his expertise in discussing hardness along different models.

### Author Statement

I declare that conceptualizations, calculations, and analyses are all mine and I have no conflict of interest with any other work or colleagues.

### Bibliography

- VV Brazhkin and VL Solozhenko. "Myths about new ultrahard phases: Why materials that are significantly superior to diamond in elastic moduli and hardness are impossible". *Journal of Applied Physics* 125, 130901 (2019).
- Shuang Shuang Zhang, *et al.* "Discovery of superhard materials via CALYPSO methodology". *Chinese Physics B* 28 (2019): 106104.
- R Hoffmann, *et al.* "Homo Citans and Carbon Allotropes: For an Ethics of Citation". *Angewandte Chemie* 55 (2016): 10962-10976. and SACADA database (Samara Carbon Allotrope Database). [www.sacada.info](http://www.sacada.info).
- SF Matar, *et al.* "The simplest dense carbon allotrope: Ultrahard body centered tetragonal C<sub>4</sub>". *Journal of Solid State Chemistry* 314 (2022): 123424.
- AP Shevchenko, *et al.* "Topological representations of crystal structures: generation, analysis, and implementation in the TopCryst system". *Science and Technology of Advanced Materials: Methods* 2.1 (2022): 250-265.
- O'Keeffe M., *et al.* "The reticular chemistry structure resource (RCSR) database of, and symbols for, crystal nets. *Acc. Chem. Res.*, 41, 1782-1789 (2008).
- P Hohenberg and W Kohn. "Inhomogeneous electron gas". *Physical Review B* 136 (1964): 864-871.
- Y Fujii, *et al.* "Pentadiamond: A Hard Carbon Allotrope of a Pentagonal Network of sp<sup>2</sup> and sp<sup>3</sup> C Atoms. *Physical Review Letters* 125 (2020): 016001 and Retraction: *Physical Review Letters* 125 (2020): 079901 (2020).
- Zhaofeng Zhai, *et al.* "Progress in electrochemistry of hybrid diamond/sp<sup>2</sup>-C nanostructures". *Current Opinion in Electrochemistry* 32 (2022): 100884.
- G Kresse and J Furthmüller. "Efficient iterative schemes for ab initio total-energy calculations using a plane-wave basis set". *Physical Review B* 54 (1996): 11169.
- G Kresse and J Joubert. "From ultrasoft pseudopotentials to the projector augmented wave". *Physical Review B* 59 (1999): 1758-1775.
- PE Blöchl. "Projector augmented wave method". *Physical Review B* 50 (1994): 17953-17979.
- J Perdew, *et al.* "The Generalized Gradient Approximation made simple". *Physical Review Letter* 77 (1996): 3865-3868.
- WH Press, *et al.* "Numerical Recipes". 2<sup>nd</sup> ed. Cambridge University Press: New York, USA, (1986).
- PE Blöchl, *et al.* "Improved tetrahedron method for Brillouin-zone integrations". *Physical Review B* 49 (1994): 16223-16233.
- M Methfessel and AT Paxton. "High-precision sampling for Brillouin-zone integration in metals". *Physical Review B* 40 (1989): 3616-3621.
- HJ Monkhorst and JD Pack. "Special k-points for Brillouin Zone integration". *Physical Review B* 13 (1976): 5188-5192.
- A Togo and I Tanaka. "First principles phonon calculations in materials science". *Scripta Materialia* 108 (2015): 1-5.
- V Eyert. "Basic notions and applications of the augmented spherical wave method". *International Journal of Quantum Chemistry* 77 (2000): 1007-1031.
- SF Matar. CCDC 2208344: (Refcode NEQHUQ; name C6POLr) (2022).

21. W Voigt. "Über die Beziehung zwischen den beiden Elastizitätsconstanten isotroper Körper". *Annals of Physics* 274 (1889): 573-587.
22. DC Wallace. "Thermodynamics of crystals". New York, USA: John Wiley and Sons (1972).
23. VA Mukhanov, *et al.* "The interrelation between hardness and compressibility of substances and their structure and thermodynamic properties". *Journal of Superhard Materials* 30 (2008): 368-378.
24. E Mazhnik and AR Oganov. "A model of hardness and fracture toughness of solids". *Journal of Applied Physics* 126 (2019): 125109.
25. AO Lyakhov and AR Oganov. "Evolutionary search for superhard materials: Methodology and applications to forms of carbon and TiO<sub>2</sub>". *Physical Review B* 84 (2011): 092103.
26. RS Krishnan. "Raman spectrum of diamond". *Nature* 155 (1945): 171.